5-31-2013

Identification of an Active Site-bound Nitrile Hydratase Intermediate through Single Turnover Stopped-flow Spectroscopy

Natalie Gumataotao
Loyola University Chicago

Misty L. Kuhn
Loyola University Chicago

Natalia Hajnas
Loyola University Chicago

Richard C. Holz
Marquette University

Published version. *Journal of Biological Chemistry*. Vol. 288, No. 22 (May 31, 2013): 15532-15536. DOI.
Richard C. Holz was affiliated with Loyola University-Chicago at the time of publication.

THE JOURNAL OF BIOLOGICAL CHEMISTRY VOL. 288, NO. 22, pp. 15532–15536, May 31, 2013

Identification of an Active Site-bound Nitrile Hydratase Intermediate through Single Turnover Stopped-flow Spectroscopy*

Received for publication, December 10, 2012, and in revised form, March 27, 2013 Published, JBC Papers in Press, April 15, 2013, DOI 10.1074/jbc.M112.398909

Natalie Gumataotao, Misty L. Kuhn, Natalia Hajnas, and Richard C. Holz[1]

From the Department of Chemistry and Biochemistry, Loyola University Chicago, Chicago, Illinois 60660

Background: No direct evidence exists for the direct coordination of nitrile to the Fe^{3+} active site in nitrile hydratases.
Results: The first Fe^{3+}-nitrile intermediate species is reported using stopped-flow spectroscopy.
Conclusion: These data establish that the direct ligation of the nitrile substrate occurs during catalytic turnover.
Significance: Understanding the catalytic mechanism of nitrile hydratases is critical to harness their bioremediation and industrial potential.

Stopped-flow kinetic data were obtained for the iron-type nitrile hydratase from *Rhodococcus equi* TG328-2 (*Re*NHase) using methacrylonitrile as the substrate. Multiple turnover experiments suggest a three-step kinetic model that allows for the reversible binding of substrate, the presence of an intermediate, and the formation of product. Microscopic rate constants determined from these data are in good agreement with steady state data confirming that the stopped-flow method used was appropriate for the reaction. Single turnover stopped-flow experiments were used to identify catalytic intermediates. These data were globally fit confirming a three-step kinetic model. Independent absorption spectra acquired between 0.005 and 0.5 s of the reaction reveal a significant increase in absorbance at 375, 460, and 550 nm along with the hypsochromic shift of an Fe^{3+}←S ligand-to-metal charge transfer band from 700 to 650 nm. The observed UV-visible absorption bands for the Fe^{3+}-nitrile intermediate species are similar to low spin Fe^{3+}-enzyme and model complexes bound by NO or N_3^-. These data provide spectroscopic evidence for the direct coordination of the nitrile substrate to the nitrile hydratase active site low spin Fe^{3+} center.

Nitrile hydratases (NHases)[2] catalyze the hydration of nitriles to their corresponding amides under ambient conditions and physiological pH (Scheme 1) (1). NHases have attracted substantial interest as biocatalysts in preparative organic chemistry and are already used in several industrial applications such as the large scale production of acrylamide (1) and nicotinamide (2). For example, Mitsubishi Rayon Co. has developed a microbial process that produces ~95,000 tons of acrylamide annually using the NHase from *Rhodococcus rhodochrous* J1 (3). More than 3,500 tons of nicotinamide are produced per year via NHase, with yields of >99% and without formation of troublesome byproducts such as acrylic acid (4). NHases have also been employed as bioremediation agents to clean up nitrile-based pesticides, such as bromoxynil (5). Because of their exquisite reaction specificity, the nitrile-hydrolyzing potential of NHase enzymes is becoming increasingly recognized as a truly new type of "green" chemistry.

NHases contain either an Fe^{3+} ion ("iron-type") or a Co^{3+} ion ("cobalt-type") in their active sites (6). X-ray crystal structures of both Co-NHase and Fe-NHase reveal that the M^{3+} ion is coordinated by three cysteines, two amide nitrogens, and a water molecule (7). Two of the active site cysteine residues are post-translationally modified to cysteine sulfinic acid ($-SO_2H$) and cysteine sulfenic acid (–SOH), yielding an unusual metal coordination geometry, termed a "claw setting." These Cys oxidation states are essential for NHase activity (8, 9).

The molecular characterization of both iron-type and cobalt-type NHase enzymes has provided some insight into how molecular structure controls enzyme function. Based on these data, and several elegant studies on active site NHase model complexes, four possible reaction mechanisms have been proposed (6, 10). In each, imidate is produced as a reaction intermediate, which then isomerizes to the corresponding amide. The most accepted catalytic mechanism for NHases involves the binding of the nitrogen of the nitrile substrate to the active site metal center; however, no direct evidence has been reported supporting such a mechanism (6, 11). Herein we report the detection of a NHase reaction intermediate, using methacrylonitrile as the substrate that is observed using stopped-flow spectroscopy. These data provide the first direct spectroscopic evidence for nitrile binding to the Fe^{3+} active site in the nitrile hydratase from *Rhodococcus equi* TG328-2 (*Re*NHase).

EXPERIMENTAL PROCEDURES

All reagents were purchased commercially and were the highest purity available.

Protein Expression—The *Re*NHase TG328-2 plasmid was kindly provided by Professor Uwe Bornscheuer (12). The sub-

* This work was supported by the National Science Foundation Grant CHE-1058357 (to R. C. H.) and American Chemical Society (ACS) Petroleum Research Fund Grant ACS PRF 50033-ND4 (to R. C. H.).
[1] To whom correspondence should be addressed: Dept. of Chemistry and Biochemistry, Loyola University Chicago, 1068 West Sheridan Rd., Chicago, Illinois 60660. Tel.: 773-508-3092; Fax: 773-508-3086; E-mail: rholz1@luc.edu.
[2] The abbreviations used are: NHase, nitrile hydratase; *Re*NHase, NHase from *R. equi*; LMCT, ligand-to-metal charge transfer.

SCHEME 1. **The hydration of a nitrile to its corresponding amide by nitrile hydratase.**

unit and activator genes were subcloned into pET-21a(+) and pET-28a(+), respectively. *Re*NHase was transformed into NEB Turbo cells (New England Biolabs) for cloning and BL21(DE3) cells (Stratagene) for protein expression. Cells were grown at 37 °C in LB media supplemented with kanamycin (50 μg/ml) and ampicillin (100 μg/ml). The cultures were cooled for 1 h upon reaching an optical density of 0.8. Cultures were induced with 0.1 mM isopropyl β-D-1-thiogalactopyranoside and 0.25 mM ferrous sulfate and shaken for an additional 16 h at 18 °C. Cells were pelleted by centrifugation at 5,000 rpm for 5 min.

Purification of ReNHase—Cells containing *Re*NHase were resuspended in 50 mM sodium phosphate buffer at pH 7.5 containing 300 mM NaCl, 40 mM butyric acid, and 10 mM imidazole at a ratio of 3 ml/g of cells and lysed by ultrasonic probe (Misonix Sonicator 3000) in 30-s increments for 4 min at 21 watts. The cell lysate was separated from cell debris by centrifugation for 40 min at 12,500 rpm and purified using immobilized metal affinity chromatography on an ÄKTA FPLC chromatographic system (GE Healthcare) at 4 °C. *Re*NHase was eluted with a linear gradient from 0 to 100% imidazole buffer (50 mM NaH_2PO_4, pH 7.5, 300 mM NaCl, 40 mM butyric acid, 500 mM imidazole) at 1 ml/min followed by buffer exchange to remove butyric acid and imidazole using an Amicon centrifugal filter unit molecular weight cut-off 30,000 (Millipore). Enzyme purity was assessed by sodium dodecyl sulfate-polyacrylamide gel electrophoresis (SDS-PAGE). A Bradford Assay was performed against bovine serum albumin (BSA) standards to determine protein concentration.

Steady State Kinetic Assay—*Re*NHase activity was examined using 100 mM methacrylonitrile as the substrate in 50 mM HEPES buffer, pH 7.0, and 25 °C at 242 nm (ϵ_{242} 3.2 mM^{-1} cm^{-1}) on a Shimadzu UV-2450 spectrometer. Initial reaction rates were monitored and fit to a modified Hill equation $y = V_{max} \times (x/(k + x))$ using Origin Pro. One unit of NHase activity was defined as the formation of 1 μmol of amide product formed per minute.

Stopped-flow Experiments—*Re*NHase activity toward methacrylonitrile was examined in triplicate using a single mixing Applied Photophysics SX-20 stopped-flow UV-visible spectrophotometer. All data were fit using Pro-Data and Pro-K software by Applied Photophysics. *Re*NHase activity was monitored at 242 nm by acquiring stopped-flow data from 0.005 to 10 s at 5 °C using 10 μM enzyme and varying concentrations of methacrylonitrile (0.1–25 mM). These data were fit to the double exponential equation.

$$Y = A_1 e^{k_{obs1} t} + A_2 e^{k_{obs2} t} + C \quad \text{(Eq. 1)}$$

Single turnover stopped-flow data were obtained using 0.33 mM *Re*NHase and 0.19 mM methacrylonitrile from 0.005 to 0.5 s.

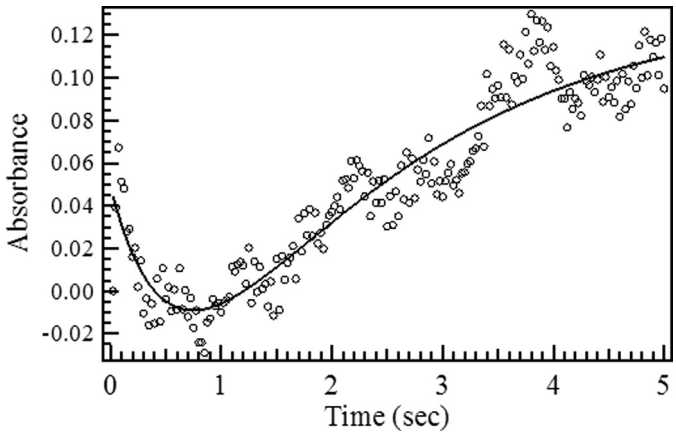

FIGURE 1. **Representative pre-steady state plot of 10 μM *Re*NHase catalyzing the hydration of 250 mM methacrylonitrile in 50 mM HEPES buffer, pH 7.0, and 5 °C at 242 nm over 0.005–5 s.**

$$E + S \underset{k_{-1}}{\overset{k_1}{\rightleftharpoons}} ES \underset{k_{-2}}{\overset{k_2}{\rightleftharpoons}} EI \xrightarrow{k_3} E + P$$

SCHEME 2. **Proposed kinetic model for the hydration of methacrylonitrile by *Re*NHase.**

Data were reduced by singular value decomposition and globally fit to various mechanistic models.

RESULTS AND DISCUSSION

Multiple turnover stopped-flow experiments were initially run at 5 °C using 25 mM methacrylonitrile at pH 7.0 (Fig. 1) to investigate pre-steady state behavior. A noticeable lag is present in the early portion of the reaction, indicating at least two reaction steps. Independent absorption spectra were acquired at 242 nm over the time frame of 0.005–10 s. These data were fit to a double exponential equation providing k_{obs1} and k_{obs2} for each phase of the reaction. k_{obs1} was designated the fast phase, and k_{obs2} was designated as the slow phase. Based on these data, a minimal three-step kinetic model is proposed that allows for reversible substrate binding, the presence of an intermediate, and the formation of product (Scheme 2).

The concentration dependence of the reaction rate on methacrylonitrile was examined by plotting the fast and slow phases (k_{obs1} and k_{obs2}) of the reaction against the substrate concentration (Fig. 2, *A* and *B*) to extract the microscopic rate constants of the reaction. The concentration dependence of the fast phase was fit to a linear equation where the slope is the second-order rate constant and the *y*-intercept is the sum of $k_{-1} + k_2 + k_{-2}$. This fit provided a k_1 value of 1.0 ± 0.1 mM^{-1} s^{-1} and a $k_{-1} + k_2 + k_{-2}$ value of 12 ± 1 s^{-1}. The nonzero intercept implies that the binding is reversible. The linear fit indicates that binding occurs in a single step (13).

The dependence of k_{obs2} on substrate was fit to a hyperbolic curve, ($k_{obs2} = k_{max}[S]/(K_{d2} + [S])$, where k_{max} is the sum of $k_2 + k_{-2}$ and is equal to the rate at saturated enzyme concentrations. K_{d2} is the apparent dissociation constant of an intermediate step following substrate binding. k_{max} was found to be 9 ± 2 s^{-1}, and K_{d2} is 1.5 ± 0.8 mM. Subtracting k_{max} ($k_2 + k_{-2}$) from the intercept of the fast phase ($k_{-1} + k_2 + k_{-2}$) provides k_{-1}, which is 3 s^{-1}. The *y*-intercept of the slow phase provides k_{-2}, which is 1 s^{-1}. Therefore, k_2 is 8 s^{-1}, and K_{d1}, which is

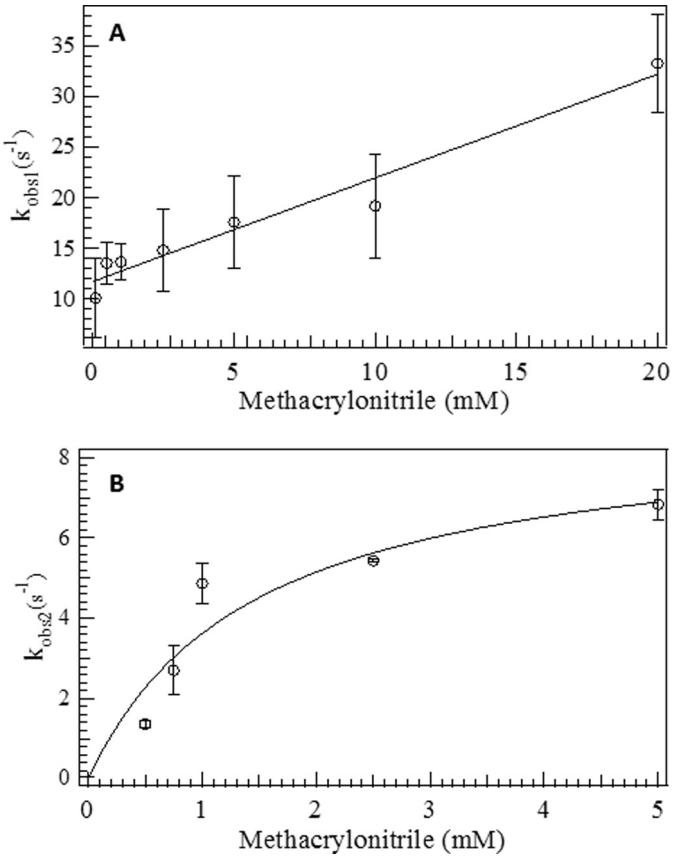

FIGURE 2. **Methacrylonitrile concentration dependence on k_{obs}.** *A*, the fast phase shows a linear dependence and a nonzero intercept, indicating a fast reversible binding step. *Error bars* indicate S.D. *B*, the slow phase exhibits a hyperbolic dependence with a maximum rate of 8 s^{-1}. *Error bars* indicate S.D.

k_{-1}/k_1, is 3 mM. The hyperbolic dependence of the slow phase indicates the presence of a second step following substrate binding, which is independent of substrate concentration.

These data were compared with experimentally determined steady state kinetic data obtained at 5 °C for *Re*NHase using 0.5–100 mM methacrylonitrile as the substrate at pH 7.0 and 242 nm. Under these conditions, the V_{max} value is 4.0 ± 0.2 s^{-1} and the K_m value is 6 ± 1 mM. One assumption under rapid equilibrium, because k_2 is greater than k_{-1}, is that K_m is greater than K_d. Therefore, the steady state K_m value of 6 mM is in good agreement with the K_d value of 3 mM determined from stopped-flow data. However, because the system is not at rapid equilibrium but at the steady state, $K_m = k_2k_3 + k_{-1}k_{-2} + k_{-1}k_3/k_1(k_2 + k_{-2} + k_3)$ for a mechanism with one intermediate before product release (14). That means the experimentally determined K_m value of 6 mM might be different from the K_d value described as k_{-1}/k_1. In our case where the values of k_1, k_{-1}, k_2, and k_{-2} were experimentally determined, K_m can only be 0.33 mM (for extremely small k_3 values) up to 11 mM (for extremely high k_3 values). For this reason, 6 mM is a value for K_m that is compatible with our measurement of the microscopic constants. In fact, values for k_3 obtained below in single turnover experiments confirm this, and these values are discussed later.

These data indicate that a three-step reaction mechanism is operative and provide microscopic rate constants. The agreement between theoretical constants calculated from the microscopic rates to steady state data also confirm that stopped-flow experiments using UV detection are valid for the NHase reaction. However, the high concentrations of substrate and subsequent product formation likely obscure potential transient intermediates. To overcome these limitations and to obtain k_3, single turnover stopped-flow experiments were performed as only kinetically significant intermediates will be observed directly.

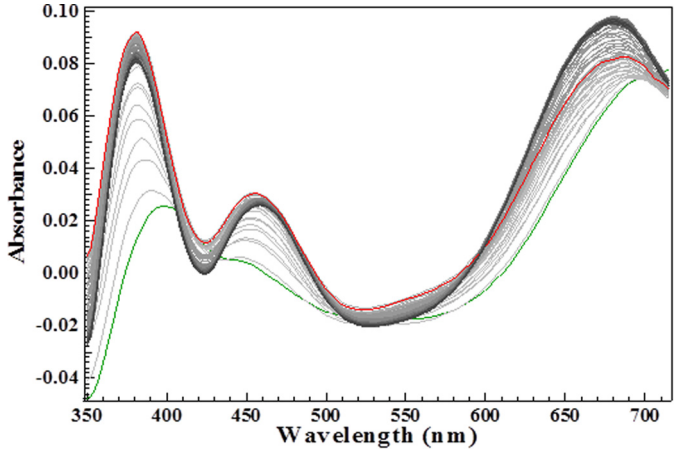

FIGURE 3. **Absorption spectra collected with mixing times ranging from 0.005 to 0.5 s for the *Re*NHase hydration reaction.** The *green line* indicates resting enzyme, whereas the *red line* is an intermediate complex. The *arrows* indicate the direction of major absorption band shifts. Experimental conditions were 0.33 mM *Re*NHase and 0.19 mM methacrylonitrile reacted in 50 mM HEPES, pH 7.0, at 25 °C.

Single turnover stopped-flow experiments are typically not feasible due to the requirement that enzyme concentrations be similar to the K_m value of the substrate. For *Re*NHase, the K_m value for methacrylonitrile is 190 μM at 25 °C, which is low enough that the enzyme can be kept at a concentration that exceeds the substrate concentration. Additionally, the *turnover* value determined at the K_m is 5 s^{-1}, placing the reaction well within the limits of the stopped-flow experiment. Therefore, independent absorption spectra were acquired between 350 and 720 nm using 0.33 mM *Re*NHase and 0.19 mM methacrylonitrile over 0.005–0.5 s of the reaction at 25 °C (Fig. 3). These transient spectra indicate the rapid formation of an Fe^{3+}-nitrile species that converts to the resting Fe^{3+} state and product. Independent spectra of enzyme intermediate complexes were extracted after singular value decomposition was applied to the raw data to eliminate noise and to isolate species with significantly different absorption spectra. In total, four species were identified as significantly different, supporting a three-step mechanism. All spectra were then globally fit using the Applied Photophysics Pro-K software to the kinetic model shown in Scheme 2. To verify that Scheme 2 was the best model, simpler and more complicated models were evaluated as well, but a three-step model provided the best global fit. To ensure that a global minimum was reached, the forward rates were varied and then verified by residual analysis, observation of positive fitted spectra, and simulation. The best fit using Scheme 2 as a model provided values for the forward rate constants k_1, k_2, and k_3 of 65 ± 10 $mM^{-1}\,s^{-1}$, 23 ± 3 s^{-1}, and 12 ± 4 s^{-1}, respectively. The reverse rate constants k_{-1} and k_{-2} were found to be 2.8 ±

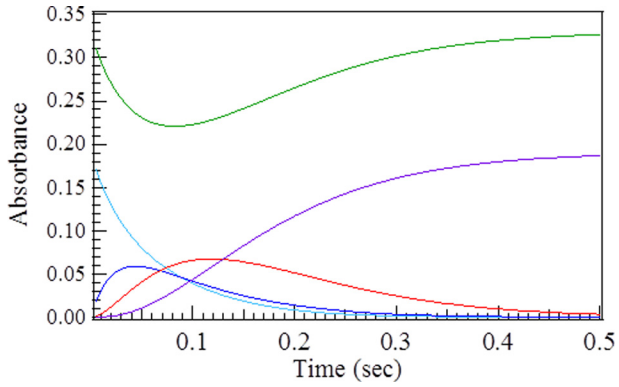

FIGURE 4. **Concentration profile of two new transient species (*red* and *blue*) observed as a function of time under single-turnover assay conditions.** The *green trace* is free enzyme, *light blue* is substrate, and *purple* is product. Conditions: 50 mM HEPES, pH 7.0, and 25 °C.

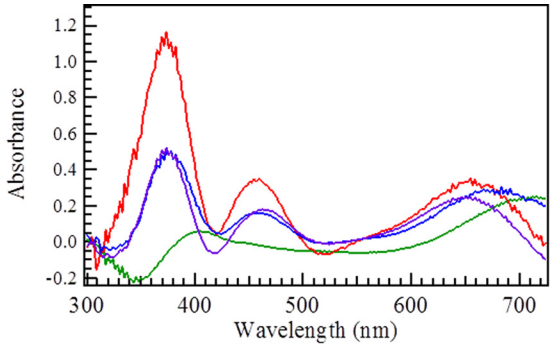

FIGURE 5. **Spectra of the intermediate species (*red* and *blue*) generated from singular value decomposition applied to the raw data and the resting enzyme (*green*) and product complex (*purple*).** Conditions: 50 mM HEPES, pH 7.0, and 25 °C.

0.1 and 1.1 ± 0.1 s^{-1}, respectively. Theoretical k_{cat} and K_m values were calculated by inserting the microscopic rate constants obtained from single turnover into the following equations derived from the minimal three-step model in Scheme 2.

$$k_{cat} = k_2k_3/k_2 + k_{-2} + k_3 \quad \text{(Eq. 2)}$$

$$K_m = k_2k_3 + k_{-1}k_{-2} + k_{-1}k_3/k_1(k_2 + k_{-2} + k_3) \quad \text{(Eq. 3)}$$

The theoretical k_{cat} and K_m values of 8 ± 3 s^{-1} and 128 ± 50 μM, respectively, are in good agreement with steady state values of 5 s^{-1} and 190 μM, respectively.

These data indicate that the substrate binding step is fast and reversible, corresponding to k_1. k_2 is the rate of rearrangement of the enzyme-substrate complex to an enzyme-product complex. Product release is rate-limiting and assigned k_3. Product release was previously shown to be rate-limiting under steady state conditions for both iron-type and cobalt-type NHase enzymes (15, 16). Concentration profiles for the progress of the reaction confirm a three-step reaction model (Fig. 4) with the observed decrease in free enzyme concentration occurring concomitantly with the formation of an enzyme-substrate complex followed by an enzyme-intermediate complex and the consumption of substrate. The first transient species reaches its maximum concentration at ~0.03 s, after which it begins to disappear, and a second transient species peaks at ~0.1 s.

Singular value decomposition identified four spectrally unique species, with one corresponding to native *Re*NHase enzyme, whereas the second is an Fe^{3+}-nitrile intermediate species (Fig. 5). As the reaction proceeds, UV-visible absorption bands appear at 375, 450, 550, and 650 nm due to an Fe^{3+}-nitrile intermediate species. These absorption bands decrease in intensity as the reaction proceeds to product with the band at 550 nm disappearing completely. Extraction of the absorption data as a function of time at 375 and 550 nm provides curves that are identical to the first and second intermediates in the concentration profile. These data are consistent with the accumulation of an Fe^{3+}-nitrile intermediate species that degrades into the resting Fe^{3+} state and product. The origin of this absorption band is likely due to an Fe^{3+}←S ligand-to-metal charge transfer (LMCT) band resulting from the strong back donation of the low spin Fe^{3+} center to the nitrile N π^* orbitals, similar to NHase-NO and Fe^{3+}-N_3^- or -NO model complexes (17–19).

Additional evidence for an Fe^{3+}-nitrile intermediate species comes from the observed absorption band at ~700 nm. In resting *Re*NHase, this band was assigned to an Fe^{3+}←S LMCT band. The observed hypsochromic shift from 700 to 650 nm upon the addition of substrate is indicative of a perturbation at the Fe^{3+} center due to nitrile binding. Blue shifts of similar magnitude have been observed in NHase enzymes and model complexes upon the addition of NO or N_3^- and were attributed to an increase in π electron donation from the axial thiolate ligand to the Fe^{3+} ion to compensate for the π-accepting behavior of the bound ligand (20, 21). Similarly, the absorbance band observed at 450 nm, which has also been assigned as an Fe^{3+}←S LMCT band based on resonance Raman data and magnetic circular dichroism model complex data (17, 19), increases in intensity upon substrate binding. Taken together, these data indicate that the observed enzyme-substrate complex is the result of the direct ligation of a nitrile to the active site low spin Fe^{3+} center, which forms an Fe^{3+}-nitrile intermediate species.

Direct ligation of a nitrile to the low spin Fe^{3+} center of *Re*NHase is also consistent with the significant increase in absorption observed at 375 nm upon the addition of methacrylonitrile to resting *Re*NHase. In the presence of NO, iron-type NHases show strong absorbance at 370 nm corresponding to an Fe^{3+}←S LMCT band that results from the direct coordination of the NO to the Fe^{3+} active site (19, 22). Direct coordination of NO to the low spin Fe^{3+} active site was confirmed by EPR and resonance Raman data, which suggested that NO displaces the axial water molecule, forming an Fe^{3+}-NO complex that is inactive. The Fe^{3+}←S LMCT band observed at ~700 nm in resting iron-type NHase is not observed in NO-inhibited NHase enzymes but reappears upon light-induced activation (19, 22). However, in the enzyme-substrate intermediate complex, the Fe^{3+}←S LMCT band at ~650 nm and a strong absorption at 375 nm are observed. This suggests that upon the addition of nitrile, the absorption band at 375 nm is due to an Fe^{3+}←S LMCT transition from nitrile coordination to the Fe^{3+} center in *Re*NHase.

The single turnover data combined with previously reported kinetic and crystallographic data allow a catalytic mechanism to be proposed for iron-type NHase enzymes that involves the

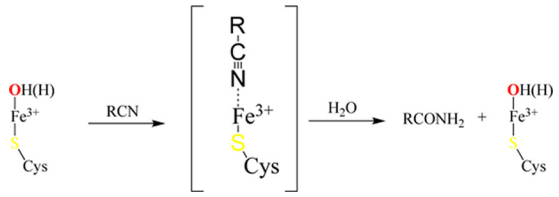

FIGURE 6. **Proposed catalytic mechanism of nitrile hydratase.**

direct ligation of the nitrile to the Fe^{3+} active site (Fig. 6) (6, 16, 22–24). The rate constants provided herein suggest a fast second-order step that involves binding of substrate to the enzyme followed by rearrangement and then product release, which is the rate-limiting step. Displacement of the metal-bound water molecule by a nitrile and coordination to the low spin Fe^{3+} center activate the CN bond toward nucleophilic attack. Once nucleophilic attack occurs followed by proton transfer, the resulting imidate can tautomerize to form an amide with a subsequent proton transfer (15, 16). Finally, the amide product can be displaced by a water molecule and thus provide the regenerated catalyst.

In conclusion, we have identified the first low spin Fe^{3+}-nitrile intermediate species for an NHase enzyme using single-turnover stopped-flow spectroscopy. The best kinetic model allows for the fast, reversible binding of substrate followed by the formation of an Fe^{3+}-nitrile intermediate species, a potential rearrangement of *ES*, and the formation of product. The product release step is rate-limiting, which is consistent with previous steady state kinetic studies for both iron-type and cobalt-type NHase enzymes (15, 16). The observed UV-visible absorption bands for an Fe^{3+}-nitrile intermediate species at 375, 450, 550, and 650 nm are similar to low spin Fe^{3+} enzyme and model complexes bound by NO or N_3^- and are indicative of strong back donation from the low spin Fe^{3+} to nitrile π^* orbitals. These data provide spectroscopic evidence for the direct ligation of the nitrile substrate to the low spin Fe^{3+} active site in NHase.

Acknowledgments—We thank Dr. Miguel Ballicora for help interpreting the kinetic component of this manuscript. We also thank Uwe T. Bornscheuer of Greifswald University for allowing the use of the His-tagged ReNHase plasmid.

REFERENCES

1. Petrillo, K. L., Wu, S., Hann, E. C., Cooling, F. B., Ben-Bassat, A., Gavagan, J. E., Dicosimo, R., and Payne, M. S. (2005) Over-expression in *Escherichia coli* of a thermally stable and regio-selective nitrile hydratase from *Comamonas testosteroni* 5-MGAM-4D. *Appl. Microbiol. Biotechnol.* **67,** 664–670
2. Padmakumar, R., and Oriel, P. (1999) Bioconversion of acrylonitrile to acrylamide using a thermostable nitrile hydratase. *Appl. Biochem. Biotechnol.* **77–79,** 671–679
3. Prasad, S., and Bhalla, T. C. (2010) Nitrile hydratases (NHases): at the interface of academia and industry. *Biotechnol. Adv.* **28,** 725–741
4. Mylerova, V., and Martinkova, L. (2003) Synthetic applications of nitrile-converting enzymes. *Curr. Org. Chem.* **7,** 1279–1295
5. Baxter, J., and Cummings, S. P. (2006) The current and future applications of microorganism in the bioremediation of cyanide contamination. *Antonie Leeuwenhoek* **90,** 1–17
6. Kovacs, J. A. (2004) Synthetic analogues of cysteinate-ligated non-heme iron and non-corrinoid cobalt enzymes. *Chem. Rev.* **104,** 825–848
7. Banerjee, A., Sharma, R., and Banerjee, U. C. (2002) The nitrile-degrading enzymes: current status and future prospects. *Appl. Microbiol. Biotechnol.* **60,** 33–44
8. Tsujimura, M., Odaka, M., Nakayama, H., Dohmae, N., Koshino, H., Asami, T., Hoshino, M., Takio, K., Yoshida, S., Maeda, M., and Endo, I. (2003) A novel inhibitor for Fe-type nitrile hydratase: 2-cyano-2-propyl hydroperoxide. *J. Am. Chem. Soc.* **125,** 11532–11538
9. Dey, A., Chow, M., Taniguchi, K., Lugo-Mas, P., Davin, S., Maeda, M., Kovacs, J. A., Odaka, M., Hodgson, K. O., Hedman, B., and Solomon, E. I. (2006) Sulfur K-edge XAS and DFT calculations on nitrile hydratase: geometric and electronic structure of the non-heme iron active site. *J. Am. Chem. Soc.* **128,** 533–541
10. Desai, L. V., and Zimmer, M. (2004) Substrate selectivity and conformational space available to bromoxynil and acrylonitrile in iron nitrile hydratase. *Dalton Trans.* **6,** 872–877
11. Wegman, M. A., van Langen, L. M., van Rantwijk, F., and Sheldon, R. A. (2002) A two-step, one-pot enzymatic synthesis of cephalexin from D-phenylglycine nitrile. *Biotechnol Bioeng.* **79,** 356–361
12. Rzeznicka, K., Schatzle, S., Bottcher, D., Klein, J., and Bornscheuer, U. T. (2010) Cloning and functional expression of a nitrile hydratase (NHase) from Rhodococcus equi TG328-2 in *Escherichia coli*, its purification and biochemical characterisation. *Appl. Microbiol. Biotechnol.* **85,** 1417–1425
13. Johnson, K. A. (1992) 1 Transient-State Kinetic Analysis of Enzyme Reaction Pathways. in *The Enzymes* (David, S. S., ed), pp. 1–61, Academic Press, San Diego, CA
14. Segel, I. H. (1993) *Enzyme Kinetics: Behavior and Analysis of Rapid Equilibrium and Steady-State Enzyme Systems*, pp. 18–72, John Wiley & Sons, Inc., New York
15. Mitra, S., and Holz, R. C. (2007) Unraveling the catalytic mechanism of nitrile hydratases. *J. Biol. Chem.* **282,** 7397–7404
16. Rao, S., and Holz, R. C. (2008) Analyzing the catalytic mechanism of the Fe-type nitrile hydratase from *Comamonas testosteroni* Ni1. *Biochemistry* **47,** 12057–12064
17. Kennepohl, P., Neese, F., Schweitzer, D., Jackson, H. L., Kovacs, J. A., and Solomon, E. I. (2005) Spectroscopy of non-heme iron thiolate complexes: insight into the electronic structure of the low-spin active site of nitrile hydratase. *Inorg. Chem.* **44,** 1826–1836
18. Rose, M. J., Betterley, N. M., Oliver, A. G., and Mascharak, P. K. (2010) Binding of nitric oxide to a synthetic model of iron-containing nitrile hydratase (Fe-NHase) and its photorelease: relevance to photoregulation of Fe-NHase by NO. *Inorg. Chem.* **49,** 1854–1864
19. Noguchi, T., Hoshino, M., Tsujimura, M., Odaka, M., Inoue, Y., and Endo, I. (1996) Resonance Raman evidence that photodissociation of nitric oxide from the non-heme iron center activates nitrile hydratase from *Rhodococcus* sp. N-771. *Biochemistry* **35,** 16777–16781
20. Sugiura, Y., Kuwahara, J., Nagasawa, T., and Yamada, H. (1987) Nitrile hydratase. The first non-heme iron enzyme with a typical low-spin iron(III)-active center. *J. Am. Chem. Soc.* **109,** 5848–5850
21. Piersma, S. R., Nojiri, M., Tsujimura, M., Noguchi, T., Odaka, M., Yohda, M., Inoue, Y., and Endo, I. (2000) Arginine 56 mutation in the β subunit of nitrile hydratase: importance of hydrogen bonding to the non-heme iron center. *J. Inorg. Biochem.* **80,** 283–288
22. Yamanaka, Y., Hashimoto, K., Ohtaki, A., Noguchi, K., Yohda, M., and Odaka, M. (2010) Kinetic and structural studies on roles of the serine ligand and a strictly conserved tyrosine residue in nitrile hydratase. *J. Biol. Inorg. Chem.* **15,** 655–665
23. Hopmann, K. H., Guo, J.-D., and Himo, F. (2007) Theoretical investigation of the first-shell mechanism of nitrile hydratase. *Inorg. Chem.* **46,** 4850–4856
24. Hashimoto, K., Suzuki, H., Taniguchi, K., Noguchi, T., Yohda, M., and Odaka, M. (2008) Catalytic mechanism of nitrile hydratase proposed by time-resolved X-ray crystallography using a novel substrate, *tert*-butylisonitrile. *J. Biol. Chem.* **283,** 36617–36623

Identification of an Active Site-bound Nitrile Hydratase Intermediate through Single Turnover Stopped-flow Spectroscopy

Natalie Gumataotao, Misty L. Kuhn, Natalia Hajnas and Richard C. Holz

J. Biol. Chem. 2013, 288:15532-15536.
doi: 10.1074/jbc.M112.398909 originally published online April 15, 2013